Ultrafast Metamorphosis of a Complex Charge-Density Wave

Kerstin Haupt,[1] Maximilian Eichberger,[2] Nicolas Erasmus,[1] Andrea Rohwer,[1] Jure Demsar,[2,3] Kai Rossnagel,[4] and Heinrich Schwoerer[1]

[1]*Laser Research Institute, Stellenbosch University, Stellenbosch 7600, South Africa*
[2]*Department of Physics, University of Konstanz, 78457 Konstanz, Germany*
[3]*Institute of Physics, Johannes Gutenberg-University Mainz, 55128 Mainz, Germany*
[4]*Institute for Experimental and Applied Physics, University of Kiel, 24098 Kiel, Germany*

(Received 11 June 2015; published 6 January 2016)

Modulated phases, commensurate or incommensurate with the host crystal lattice, are ubiquitous in solids. The transition between such phases involves formation and rearrangement of domain walls and is generally slow. Using ultrafast electron diffraction, we directly record the photoinduced transformation between a nearly commensurate and an incommensurate charge-density-wave phase in $1T$-TaS_2. The transformation takes place on the picosecond time scale, orders of magnitude faster than previously observed for commensurate-to-incommensurate transitions. The transition speed and mechanism can be linked to the peculiar nanoscale structure of the photoexcited nearly commensurate phase.

DOI: 10.1103/PhysRevLett.116.016402

Complex intertwined electronic and lattice orders are a hallmark of strongly correlated materials. Prominent examples include the plethora of charge-density-wave (CDW) phases in layered compounds [1], the strongly coupled electronic and lattice orders involved in the metal-insulator transitions of VO_2 [2,3] and Fe_3O_4 [4], and the combined charge, orbital, and lattice orders in manganites [5]. The spatial structures range from homogeneous commensurate and incommensurate phases over domain structures to local short-range order on the nanometer length scale. The understanding of these orders and the transitions between them is an important step towards understanding strongly correlated materials in general and harnessing their properties.

In recent years, femtosecond time-resolved spectroscopy [6–18] and diffraction techniques [19–26] have contributed many important insights into the nature and origin of electronic (charge, orbital, spin) and lattice orders. Intense femtosecond optical pulses, with carrier frequencies ranging from terahertz [6,7,24] to ultraviolet, are usually used to perturb the low-temperature ground state and the resulting dynamics are probed by tracking the time evolution of the system in a stroboscopic fashion. By selectively probing the dynamics of the electronic and lattice subsystems, their coupling strengths can be determined [8,9], providing insights into the ground states and opening new pathways for controlling macroscopic orders [6,7,10,11,24,25]. In a large majority of these studies, the low-temperature order is quenched at high enough excitation densities, and studies focus on its melting [7,14,15,20–25], switching [9–11,17,24] and/or recovery dynamics [8,13,16,21]. In some cases, however, new transient [6,10] or metastable [17] orders can be induced by light excitation.

In this Letter, we report an ultrafast electron diffraction study, where we directly follow the genesis of a strongly coupled electronic and structural order: the emergence of an incommensurate (IC) CDW out of a nearly commensurate (NC), domainlike CDW in $1T$-TaS_2, a drosophila of ultrafast dynamics [12,13,16,17,20,26]. We initiate the phase transformation from the NC phase at $T = 305$ K by exciting a ~22 nm thin $1T$-TaS_2 crystal with an ultrashort laser pulse. At subsequent delay times we monitor both the suppression of the NC and the emergence of the IC order in real time by capturing their structural fingerprints in electron diffraction patterns. The experimental results provide clear evidence that the phase transition follows a multistep process: after a subpicosecond suppression of the NC order, the new IC order nucleates at the original domain walls of the NC phase within about 2 ps and grows into the NC domains on the 10–100 ps time scale. Such transitions, involving rearrangement of domain structure [27,28] in macroscopic samples, should generally be slow. Indeed, electric field-driven commensurate-to-incommensurate transitions in ferroelectrics take place on a millisecond time scale [29,30]. The dramatic difference in time scales observed in this work is attributed to the peculiar nanoscale structure of the NC phase.

$1T$-TaS_2 provides a classic example of how complex forms of coupled electronic and structural orders can emerge from a simple layered structure. The phase diagram of the pristine compound comprises a commensurate (C) CDW coupled to a Mott insulating phase [31–33] at low temperatures, stripelike and NC phases at intermediate, and an IC phase at high temperatures [27,28]. Upon intercalation, transition-metal substitution, and hydrostatic pressure, several additional CDW phases come up, some of them even coexisting with superconductivity [34–36].

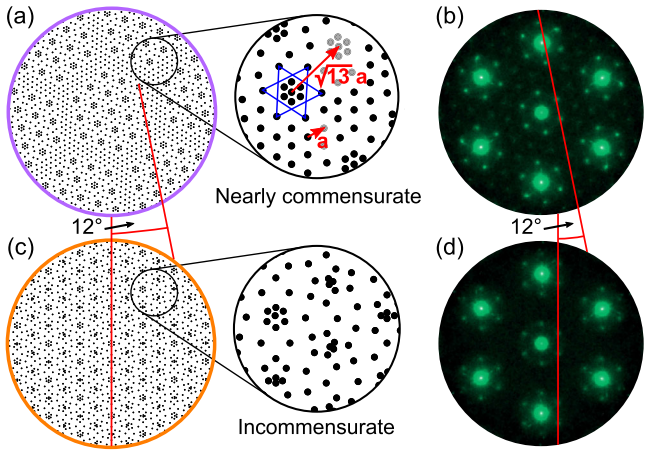

FIG. 1. Real (a),(c) and reciprocal (b),(d) space representations of the NC and IC phases of 1T-TaS_2. (a) Simplified model of the NC phase in real space: Commensurate domains of 13-atom clusters in a $\sqrt{13} \times \sqrt{13}$ superstructure are separated by unmodulated domain walls [28]. Modulation amplitudes are exaggerated for visual clarity. (b) The corresponding transmission electron diffraction pattern. Bright diffraction peaks represent the host crystal lattice, weaker satellite peaks with relative intensity of 6% are the signature of the NC phase. Note the 12° angle between the peaks of the crystal lattice and superstructure, distinctly different from the 13.9° angle of the C phase. (c) Visualization of the IC phase in real space. The hexagonal lattice is modulated by three harmonic modulations (wavelength 3.53a) along the three lattice vectors at 120°. Phases of the three harmonics are set to zero at the center of the figure. (d) The diffraction pattern of the IC phase. The superlattice peaks of about 3% relative intensity are aligned with the lattice diffraction pattern.

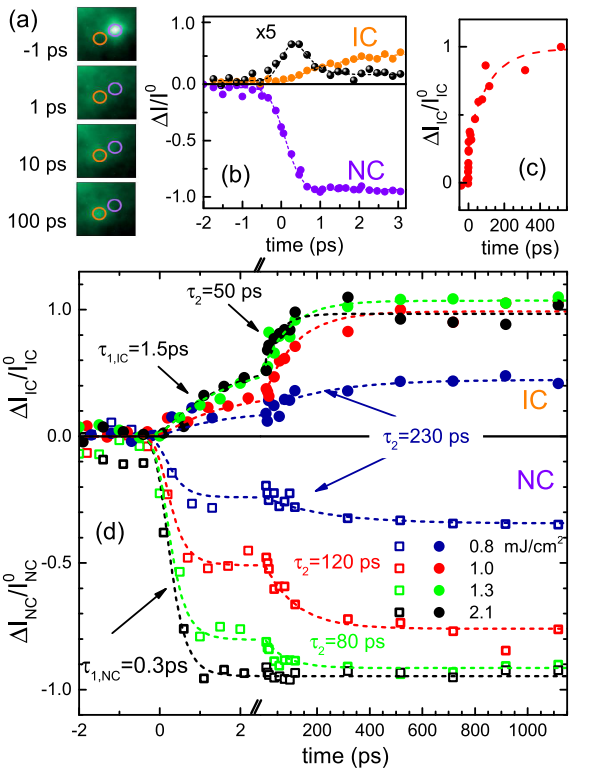

FIG. 2. NC-to-IC transformation recorded at different excitation densities. (a) Snapshots of diffraction intensity near the superlattice reflection (zoom-in) at several time delays after excitation with 1.9 mJ/cm^2. (b) The corresponding time evolution of diffraction intensities (black symbols represent the intensity of the main lattice peaks). (c) The time evolution of intensity of the IC peak (1 mJ/cm^2), displaying a two-step process. (d) The evolution of the NC and IC intensities for different excitation densities. Characteristic time scales are shown (see text). The second stage of the photoinduced transformation proceeds on an excitation density-dependent time scale (τ_2), describing both, further NC suppression and IC growth. τ_2 ranges from ≈230 ps at 0.8 mJ/cm^2 to ≈50 ps at 2.1 mJ/cm^2.

Here, we focus on the first-order phase transition [37,38] from the NC to the IC order at $T_{NI} = (353 \pm 1)$ K in pristine 1T-TaS_2. We note that the photoinduced phase transition was (at least partially) realized in Ref. [20], yet the data quality was insufficient to track its time evolution.

The NC phase exhibits an intriguing nanometer-scale inhomogeneity in real space: it can be approximated as consisting of small domains of commensurate 13-atom clusters, separated by several atoms wide discommensurations (domain walls), where modulation is negligible [Fig. 1(a)] [27,28,39]. The volume fraction of discommensurations is about 50%. The IC phase, on the other hand, is spatially homogeneous but not in registry with the underlying lattice [Fig. 1(c)]. The two phases differ in reciprocal space, as demonstrated in the transmission electron diffraction images in Figs. 1(b) and 1(d) recorded with our femtosecond electron diffraction setup. The CDW fingerprints are the weak hexagonal patterns surrounding the strong diffraction peaks of the underlying hexagonal crystal structure. Whereas the IC signature is in line with the reciprocal crystal pattern, the NC signature is rotated by ∼12° and also expresses higher order diffraction peaks.

The temperature dependences of the superlattice peak intensities in the vicinity of T_{NI}, recorded with our setup and shown in Fig. S1 [40], display the steplike characteristics of the first-order phase transition. The intensity of the IC peak well in the incommensurate phase, I^0_{IC}, is about one-half of the intensity of the NC peak at room temperature, I^0_{NC}. This value reflects the reduced CDW amplitude and a different structure factor of the IC phase [32,41].

All transient electron diffraction experiments were performed at room temperature [40]. The overall experimental temporal resolution was about 600 fs, with the electron transverse coherence length of more than 8 nm [40] sufficient to identify the different superstructures.

Figure 2(a) shows diffraction snapshots at several time delays after excitation with a 150 fs near-infrared pulse with an incoming fluence $F = 1.9$ mJ/cm^2. As shown in Fig. 2(b) the intensity of the NC peak, I_{NC}, drops to zero on

the sub-ps time scale. By assuming an exponential process [40], we estimate the time constant to be $\tau_{1,NC} \approx 0.3$ ps, ascribed to the "coherent" initial suppression of the NC order [20]. This coherent process, accompanied by a rapid electron-phonon thermalization on a time scale $\tau_{DW} \approx 1$ ps, accounts well for the time evolution of the intensity of the main lattice peak (black symbols). In addition to the two signatures, whose time evolutions in the perturbative regime were reported in Ref. [20], we observed the buildup of the IC phase. The intensity of the IC peak, I_{IC}, is found to reach about 50% of I_{IC}^0 on a time scale of $\tau_{1,IC} \approx 1.5$ ps. However, the growth of I_{IC} continues up to ≈100 ps reaching I_{IC}^0. The snapshot of diffraction taken 100 ps after photoexcitation is identical in angular orientation and intensity to that of a sample thermally heated above T_{NI}, demonstrating the phase transformation is complete. Unlike in the recently reported low temperature (<50 K) phase [17], the system then cools back to its initial NC state before the arrival of the next pump pulse (1 ms). We emphasize that during the photoinduced NC-to-IC transition the CDW diffraction peaks do not rotate. Following quenching of the NC order within τ_1 the I_{IC} signal starts to grow. As shown in Fig. S4 [40], the width of the IC peak is initially about a factor of 2 larger than in thermal equilibrium, denoting a shorter correlation length. At 100 ps, however, its width already matches the one of the lattice reflections, implying the correlation length of the IC order comparable to or larger than the transverse coherence length of our electron pulse (8 nm).

This multistep phase transformation is further elucidated in Figs. 2(c) and 2(d) showing the time evolutions of I_{NC} and I_{IC} for incident laser fluences between 0.8 and 2.1 mJ/cm^2. Interestingly, for $0.8 < F < 1.3$ mJ/cm^2 even I_{NC} is found to follow a two-step process. Assuming the processes to follow exponential time dependences, all data can be fit (dashed lines) by considering $\tau_{1,NC} = 0.3$ ps, $\tau_{DW} = 1$ ps, $\tau_{1,IC} = 1.5$ ps to be independent on F. However, the time scale τ_2, describing the second stage of the growth (suppression) of $I_{IC}(I_{NC})$, is found to vary between ≈230 ps and ≈50 ps, decreasing with increasing F.

Important clues about the nature of the photoinduced phase transition can be gained from the energetics of the process. To estimate the absorbed energy density, we combined spectroscopic ellipsometry on a bulk crystal with measurements of the optical transmission and reflectivity of the free-standing film and determined that the excitation profile over the 100 μm × 100 μm × 22 nm sample volume is homogeneous within 10% (see Fig. S2 [40]). Because of the fast electron-phonon thermalization ($\tau_{DW} \approx 1$ ps), a quasiequilibrium between the electronic and lattice systems will be reached within a few picoseconds. To estimate the resulting quasiequilibrium temperature, T^*, we used the calculated absorbed energy density and the known values of the (total) specific heat, including the phase transition enthalpy [42].

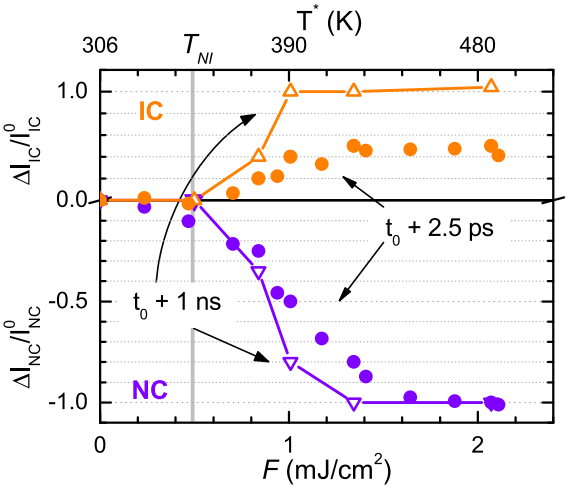

FIG. 3. NC and IC intensities at the time delay of 2.5 ps (solid circles) and 1 ns (open triangles) as a function of F and the corresponding quasiequilibrium temperature T^*. The gray line represents the equilibrium transition temperature T_{NI}. For $F \lesssim 0.5$ mJ/cm^2 no signature of the IC phase is observed.

Figure 3 shows relative changes of NC and IC intensities at two specific pump-probe delays, 2.5 ps and 1 ns, as a function of F (bottom axis) and the calculated T^* (top axis). No signature of the photoinduced *IC* order is observed for $F \leq 0.5$ mJ/cm^2, whereby the corresponding T^* reaches T_{NI}. This indicates that the sample is superheated during the photoinduced phase transition, similar to transient melting of ice [43]. Moreover, for $F > 1.0$ mJ/cm^2 the phase transition is completed after τ_2, while for $F = 0.8$ and 1.0 mJ/cm^2 the crystal remains in a mixed phase even at 1 ns after photoexcitation. Finally, comparing the relative I_{IC} intensities at the delays of 2.5 ps and 1 ns shows that their ratio is roughly 1:2 for fluences higher than 1 mJ/cm^2.

From the equilibrium atomic positions of the NC and IC phases (Fig. 1) it follows that the phase transformation cannot proceed coherently, as one may expect for the transition between a (commensurately) modulated and a nonmodulated phase [25]. In other words, the two phases are not linked by a generalized coordinate, and we neither have access to the atomic trajectories, nor to the transient potential energy surfaces along which the atoms move. This is consistent with the observation that even the formation time $\tau_{1,IC}$ is substantially longer than $\tau_{1,NC}$ and the melting time τ_{DW}.

The observed two-stage buildup of the IC phase seems consistent with the general features of driven first-order phase transitions [44], where nucleation of the new phase is followed by the domain growth, as, e.g., in the classic case of quenching a binary mixture into the metastable state between the binodal and spinodal curves [44,45]. The fact that the correlation length of the IC phase grows during the second stage (Fig. S4 [40]) is also consistent with the domain growth. The nucleation process is commonly associated with a nucleation barrier, implying the

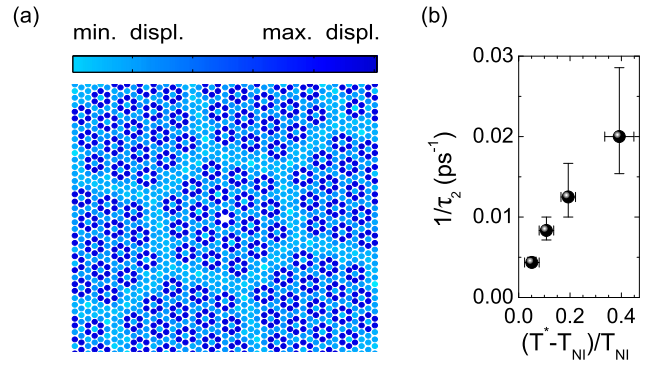

FIG. 4. (a) Average displacement amplitude for a NC-to-IC phase transition. Solid circles represent the atomic positions of the hexagonal host lattice; the color coding indicates how much on average (considering that the IC modulation is not in registry with the host lattice) each atom needs to move starting from its NC position to arriving at its IC position (see Ref. [40]). Atoms within the discommensurations are on average much closer to their end positions. (b) The transformation rate τ_2^{-1} as a function of reduced temperature ($T^* - T_{NI}$).

dependence of the nucleation rate on excitation density (or T^*), which is not observed here. Moreover, the initial buildup of the IC phase, proceeding on the time scale $\tau_{1,IC}$, matches the characteristic phonon time scales. These two observations imply the absence of a nucleation barrier in the photoinduced NC -to-IC transition, as in the case of spinodal decomposition following a rapid quench [44,45].

To gain further insight into the photoinduced NC-to-IC transition, we have calculated the average net displacements of Ta atoms upon the transition from the NC phase into the high-temperature IC phase [40]. The result, shown in Fig. 4(a) (see also Fig. S3 [40]), reveals that atoms within the discommensuration regions (domain walls) are on average much closer to their final positions than atoms within the commensurate domains. Moreover, the volumes of discommensurations and commensurate domains in the NC phase around room temperature are roughly equal [27,28]. Thus, we propose the following scenario: The femtosecond laser excitation of the electronic system and the resulting changes in the ionic potential launch coherent atomic motion in the commensurate domains towards the undistorted metallic phase. On a similar time scale ($\tau_{DW} \approx 1$ ps) the energy is dissipated to the lattice, resulting in a quasithermalized electron and lattice system at $T^* > T_{NI}$. Within the discommensurations, taking up about one-half of the sample volume, the lattice has to restructure only slightly, and these areas develop the IC order within picoseconds, consistent with the absence of a nucleation barrier.

Following the "nucleation," further growth of the IC phase requires the transformation of the previously commensurate domains. Here, the necessary atomic displacements are much larger. Moreover, phase coherence needs to be established over sizable areas. As demonstrated in Fig. 2(d), the time scale of this process, τ_2, depends on F (or T^*). It shows slowing down as T^* approaches T_{NI}. Most interestingly, the rate τ_2^{-1} is found to scale with the reduced temperature, $T^* - T_{NI}$, as shown in Fig. 4(b). While such a critical behavior is expected for continuous phase transitions, similar observations have been made for first-order phase transitions in ferroelectrics [46], albeit for temperatures much closer to the phase transition temperature [29,30] compared to our case.

Overall, our results reveal an excitation density-dependent multistage NC-to-IC phase transformation that, at the highest excitation density used here, completes within ~50 ps. This transformation time is orders of magnitude faster than the ones reported previously for electric field-driven commensurate-to-incommensurate transitions in ferroelectrics [29,30]. In fact, even if we extrapolate τ_2^{-1} to reduced temperatures, comparable to the ones used in experiments on ferroelectrics (≈2 K) [29,30,46], the phase transformation in our case proceeds about 4 orders of magnitude faster. We attribute this to the peculiar nanoscale structure of the NC phase. Indeed, for the highest excitation densities, τ_2^{-1} approaches the ultimate time scale for a buildup of new long-range structural order, which is limited by the characteristic length scale of the NC phase (5 nm [27]) and the sound velocity (~10^3 m/s [47]) to a few picoseconds. This is consistent with the earlier study [20], where for substantially higher fluences the phase transition was realized, yet not resolved in time.

The mechanism of the photoinduced phase transition followed here is distinctly different from that of the thermally driven equilibrium phase transition [27,28]. In the equilibrium NC-to-IC transition of 1T-TaS_2, as in commensurate-to-incommensurate transitions in general [48,49], the commensurate domains successively melt into a finer, denser network structure of discommensurations [27,28]. By contrast, our measurements suggest that the photoinduced transformation proceeds via a broadening of the network structure. Since the symmetric CDW amplitude mode of the 13-atom clusters in the commensurate domains does not directly map onto the distortion pattern of the IC phase, this appears as the fastest possible pathway.

These results establish one of the fastest transitions between two quantum phases with distinct macroscopic orders. As such they provide a reference for how and how fast complex nanoscale structural orders can be transformed. The proposed mechanism and characteristic time scales could be relevant whenever there is no direct "coherent" path between the initial and final phase of a photoinduced transition. From an experimental point of view, our results open an intriguing perspective on the study of strongly correlated materials. In ultrafast electron diffraction, information about structural dynamics over the entire two-dimensional Brillouin zone is obtained in a single run. Thus, one can envisage the use of ultrafast electron diffraction in finding signatures of transient or

fluctuating orders. Indeed, with constantly improving sensitivity, such experiments are becoming feasible.

We would like to acknowledge discussions with K. Binder, T. Palberg, V. V. Kabanov, B. Rethfeld, and P. Leiderer, and thank S. Shokhovets for performing spectroscopic ellipsometry measurements. M. E. acknowledges financial support through a Stiftung der Deutschen Wirtschaft (sdw) scholarship. This work is based upon research supported by the South African Research Chair Initiative of the Department of Science and Technology and the National Research Foundation.

[1] J. A. Wilson, F. J. Di Salvo, and S. Mahajan, Adv. Phys. **24**, 117 (1975).
[2] J. B. Goodenough, J. Solid State Chem. **3**, 490 (1971).
[3] A. Zylbersztejn and N. F. Mott, Phys. Rev. B **11**, 4383 (1975).
[4] E. J. W. Verwey, Nature (London) **144**, 327 (1939).
[5] E. Dagotto, Science **309**, 257 (2005).
[6] D. Fausti, R. I. Tobey, N. Dean, S. Kaiser, A. Dienst, M. C. Hoffmann, S. Pyon, T. Takayama, H. Takagi, and A. Cavalleri, Science **331**, 189 (2011).
[7] M. Liu *et al.*, Nature (London) **487**, 345 (2012).
[8] H. Schäfer, V. V. Kabanov, M. Beyer, K Biljakovic, and J. Demsar, Phys. Rev. Lett. **105**, 066402 (2010).
[9] I. Radu *et al.*, Nature (London) **472**, 205 (2011).
[10] K. W. Kim, A. Pashkin, H. Schäfer, M. Beyer, M. Porer, T. Wolf, C. Bernhard, J. Demsar, R. Huber, and A. Leitenstorfer, Nat. Mater. **11**, 497 (2012).
[11] T. Q. Li, A. Patz, L. Mouchliadis, J. Yan, Th. Lograsso, I. Perakis, and J. Wang, Nature (London) **496**, 69 (2013).
[12] J. Demsar, L. Forró, H. Berger, and D. Mihailovic, Phys. Rev. B **66**, 041101(R) (2002).
[13] L. Perfetti, P. A. Loukakos, M. Lisowski, U. Bovensiepen, H. Berger, S. Biermann, P. S. Cornaglia, A. Georges, and M. Wolf, Phys. Rev. Lett. **97**, 067402 (2006).
[14] F. Schmitt *et al.*, Science **321**, 1649 (2008).
[15] T. Rohwer *et al.*, Nature (London) **471**, 490 (2011).
[16] N. Dean, J. C. Petersen, D. Fausti, R. I. Tobey, S. Kaiser, L. V. Gasparov, H. Berger, and A. Cavalleri, Phys. Rev. Lett. **106**, 016401 (2011).
[17] L. Stojchevska, I. Vaskivskyi, T. Mertelj, P. Kusar, D. Svetin, S. Brazovskii, and D. Mihailovic, Science **344**, 177 (2014).
[18] M. Porer, U. Leierseder, J.-M. Ménard, H. Dachraoui, L. Mouchliadis, I. E. Perakis, U. Heinzmann, J. Demsar, K. Rossnagel, and R. Huber, Nat. Mater. **13**, 857 (2014).
[19] V. A. Lobastov, R. Srinivasan, and A. H. Zewail, Proc. Natl. Acad. Sci. U.S.A. **102**, 7069 (2005).
[20] M. Eichberger, H. Schfer, M. Krumova, M. Beyer, J. Demsar, H. Berger, G. Moriena, G. Sciaini, and R. Miller, Nature (London) **468**, 799 (2010).
[21] N. Erasmus, M. Eichberger, K. Haupt, I. Boshoff, G. Kassier, R. Bimurske, H. Berger, J. Demsar, and H. Schwoerer, Phys. Rev. Lett. **109**, 167402 (2012).
[22] S. de Jong *et al.*, Nat. Mater. **12**, 882 (2013).
[23] M. Gao *et al.*, Nature (London) **496**, 343 (2013).
[24] T. Kubacka *et al.*, Science **343**, 1333 (2014).
[25] T. Huber *et al.*, Phys. Rev. Lett. **113**, 026401 (2014).
[26] T. Han, F. Zhou, Ch. Malliakas, P. Duxbury, S. Mahanti, M. Kanatzidis, and C.-Y. Ruan, Sci. Adv. **1**, e1400173 (2015).
[27] T. Ishiguro and H. Sato, Phys. Rev. B **44**, 2046 (1991).
[28] T. Ishiguro and H. Sato, Phys. Rev. B **52**, 759 (1995).
[29] K. Hamano, H. Sakata, and K. Ema, J. Phys. Soc. Jpn. **54**, 2021 (1985).
[30] K. Elisbihani, H. Gibhardt, and G. Eckold, Phys. Chem. Chem. Phys. **11**, 3168 (2009).
[31] P. Fazekas and E. Tosatti, Philos. Mag. B **39**, 229 (1979).
[32] R. Brouwer and F. Jellinek, Physica (Amsterdam) **99B**, 51 (1980).
[33] K. Rossnagel and N. V. Smith, Phys. Rev. B **73**, 073106 (2006).
[34] W. Clark and P. M. Williams, Philos. Mag. **35**, 883 (1977).
[35] B. Sipos, A. Kusmartseva, A. Akrap, H. Berger, L. Forr, and E. Tutis, Nat. Mater. **7**, 960 (2008).
[36] L. J. Li, W. J. Lu, X. D. Zhu, L. S. Ling, Z. Qu, and Y. P. Sun, Europhys. Lett. **97**, 67005 (2012).
[37] S. Bayliss, A. Ghorayeb, and D. Guy, J. Phys. C **17**, L533 (1984).
[38] R. E. Thomson, U. Walter, E. Ganz, J. Clarke, A. Zettl, P. Rauch, and F. J. DiSalvo, Phys. Rev. B **38**, 10734 (1988).
[39] A. Spijkerman, J. L. de Boer, A. Meetsma, G. A. Wiegers, and S. van Smaalen, Phys. Rev. B **56**, 13757 (1997).
[40] See Supplemental Material at http://link.aps.org/supplemental/10.1103/PhysRevLett.116.016402 for additional information on sample preparation, diffraction experiments, data analysis, and simulation results.
[41] L. D. Chapman and R. Colella, Phys. Rev. Lett. **52**, 652 (1984).
[42] A. Suzuki, M. Koizumi, and M. Doyama, Solid State Commun. **53**, 201 (1985).
[43] H. Iglev, M. Schmeisser, K. Simeonidis, A. Thaller, and A. Laubereau, Nature (London) **439**, 183 (2006).
[44] P. Papon, J. Leblond, and P. Meijer, *The Physics of Phase Transitions* (Springer Verlag, New York, 2006).
[45] K. Binder, Rep. Prog. Phys. **50**, 783 (1987).
[46] K. Hamano, H. Sakata, and K. Ema, Ferroelectrics **137**, 235 (1992).
[47] M. Skolnick, S. Roth, and H. Alms, J. Phys. C **10**, 2523 (1977).
[48] W. McMillan, Phys. Rev. B **14**, 1496 (1976).
[49] P. Bak, Rep. Prog. Phys. **45**, 587 (1982).